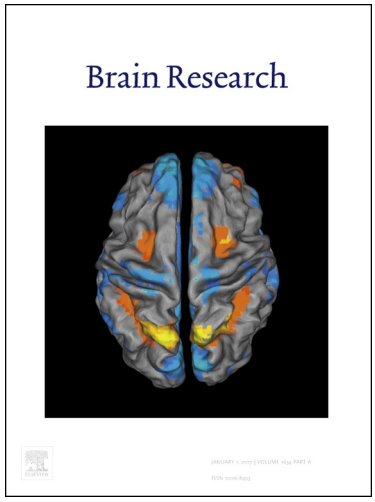

Research report

Sab is differentially expressed in the brain and affects neuronal activity

Alejandro O. Sodero, Monica Rodriguez-Silva, Chiara Salio, Marco Sassoè-Pognetto, Jeremy W. Chambers

PII: S0006-8993(17)30248-2
DOI: http://dx.doi.org/10.1016/j.brainres.2017.06.005
Reference: BRES 45387

To appear in: *Brain Research*

Received Date: 23 November 2016
Revised Date: 1 June 2017
Accepted Date: 3 June 2017

Please cite this article as: A.O. Sodero, M. Rodriguez-Silva, C. Salio, M. Sassoè-Pognetto, J.W. Chambers, Sab is differentially expressed in the brain and affects neuronal activity, *Brain Research* (2017), doi: http://dx.doi.org/10.1016/j.brainres.2017.06.005

Sab is differentially expressed in the brain and affects neuronal activity.

Alejandro O. Sodero[1], Monica Rodriguez-Silva[1], Chiara Salio[3], Marco Sassoè-Pognetto[4] and Jeremy W. Chambers[1,2*]

[1]Department of Cellular Biology and Pharmacology, [2]Department of Neuroscience, Herbert Wertheim College of Medicine, Florida International University, Miami, FL 33199.

[3]Department of Veterinary Sciences, [4]Department of Neuroscience, University of Turin, Italy.

*Corresponding Author: Jeremy W. Chambers, Ph.D., Assistant Professor

Herbert Wertheim College of Medicine

Florida International University

AHC4, Room 232

11200 SW 8th Street

Miami, FL 33199

Office: (305) 348-4648

Email: jwchambe @fiu.edu

Running Title: Sab-mediated signaling facilitates neuronal activity

Abstract

Sab (SH3 binding protein 5 or SH3BP5) is a mitochondrial scaffold protein involved in signaling associated with mitochondrial dysfunction and apoptosis; furthermore, Sab is a crucial signaling platform for neurodegenerative disease. To determine how this signaling nexus could have a significant effect on disease, we examined the regional abundance of Sab in the brain and sub-neuronal distribution, and we monitored the effect of Sab-mediated signaling on neuronal activity. We found that Sab is widely expressed in the adult mouse brain with increased abundance in hippocampus, ventral midbrain, and cerebellum. Sab was found in purified synaptosomes and in cultures of hippocampal neurons and astrocytes. Confocal and electron microscopy of mouse hippocampal sections confirmed the mitochondrial localization of Sab in the soma, dendrites, and axons. Given the localization and sub-neuronal distribution of Sab, we postulated that Sab-mediated signaling could affect neuronal function, so we measured the impact of inhibiting Sab-mediated events on the spontaneous activity in cultured hippocampal neurons. Treatment with a Sab-inhibitory peptide (Tat-Sab_{KIM1}), but not a scrambled control peptide, decreased the firing frequency and spike amplitudes. Our results demonstrate that brain-specific Sab-mediated signaling plays a role in neuronal activity through the manipulation of mitochondrial physiology by interacting kinases.

Keywords

Hippocampus, Mitogen-activated Protein Kinase, Neuron, Sab, Signal Transduction

1. Introduction

Mitogen-activated protein kinases (MAPKs) are emerging as critical regulators of neuronal function and disease. The c-Jun N-terminal kinase (JNK) is a serine/threonine MAPK that is highly expressed and very active in the brain (Brecht et al., 2005; Carboni et al., 1998; Hu et al., 1997; Lee et al., 1999; Lundby et al., 2012) . In fact, JNK isoforms are extensively linked to neuronal development, function, and disease (Coffey, 2014). This diversity of function can be attributed to the fact that there are three (3) JNK isoforms in the brain (JNK1, JNK2, and JNK3), which can be further processed into ten (10) distinct variants (Gupta et al., 1996). The isoforms specifically vary in their tissue and subcellular distributions as well. The JNK1 isoform accounts for most of the JNK activity in the cortex and cerebellum (Tararuk et al., 2006); meanwhile, JNK3 activity dominates in the hippocampus and striatum (Brecht et al., 2005). In neurons, JNK1 is found predominantly in the cytosol, while JNK3 is largely nuclear; JNK2, which exhibits the lowest expression in the brain, is distributed between the nucleus and cytosol (Lee et al., 1999). However, subcellular isoform distribution can vary within specific regions of the brain depending on the relative abundance of specific JNK isoform expression in each area.

In the adult brain, JNK signaling affects macromolecular transport and synaptic plasticity. JNK interacts with vesicular structures and binds to microtubule-associated proteins in the brain (Bjorkblom et al., 2005; Cavalli et al., 2005; Coffey et al., 2000; Feltrin et al., 2012; Tararuk et al., 2006). Collectively, these studies indicate that JNK signaling plays a role in vesicle trafficking and deployment during neurotransmission. Furthermore, JNK1-deficient mice have diminished long-term depression, while JNK2-null mice have reduced late phase long-term potentiation (Chen et al., 2005; Li et al., 2007). Additionally, JNK1-deficient mice or mice treated with JNK-selective inhibitors have decreased basal synaptic transmission (Li et al., 2007;

Yang et al., 2011). These studies demonstrate an importance for JNK signaling in neurotransmission.

Efficient neurotransmission in the adult brain requires proper levels of adenosine triphosphate (ATP) and its generation relies on healthy mitochondria. Indeed, perturbations in mitochondrial function are postulated to precede the onset of cognitive decline and neurodegenerative disease (Knott et al., 2008; Lin and Beal, 2006). Consequently, molecular mechanisms regulating mitochondrial physiology have been shown to play crucial roles in neurotransmission as well as neurological disease (Ivannikov et al., 2013; Small et al., 2011). While the impact of nuclear and cytosolic JNK activities are documented in the brain, less is known regarding mitochondrial JNK activity in the brain under physiological conditions (Coffey, 2014). Sab (SH3 binding protein 5 or SH3BP5) is a scaffold protein present at mitochondria that facilitates MAPK signaling on the organelle (Chambers et al., 2011a; Wiltshire et al., 2004). This subcellular location favors the interaction of Sab with cytoplasmic proteins involved in different signal transduction pathways, facilitating the communication between mitochondria and the rest of the cell. Specifically, the C-terminal portion of Sab contains two kinase interaction motifs (KIMs) possessing consensus binding sites for MAPKs (Wiltshire et al., 2002). Indeed, Sab interacts with JNK in response to distinct cellular stimuli, including neurotoxic chemicals (Aoki et al., 2002; Chambers et al., 2013; Win et al., 2011; Win et al., 2014).

There is little information regarding the physiological role of mitochondrial JNK signaling in the adult brain, as most of the studies have focused on the stress responsiveness and disease-specific contexts of mitochondrial JNK. In response to neurological stress, JNK translocates to mitochondria and phosphorylates Bcl-2 family proteins; specifically, Bcl-2 like protein 11 (Bim) and the BH-3 only protein hara-kiri (Hrk) are phosphorylated by JNK during

serum or nerve growth factor withdrawal as well as during ischemia (Harris and Johnson, 2001; Lei and Davis, 2003; Putcha et al., 2001; Putcha et al., 2003). We have demonstrated that mitochondrial JNK signaling can be selectively inhibited by specifically targeting the JNK-Sab interaction. Using a small, cell-permeable peptide (Tat-Sab_{KIM1}) to emulate the JNK binding site on Sab, we blocked mitochondrial JNK signaling and prevented stress-induced apoptosis without disrupting nuclear JNK activity (Chambers et al., 2011a). We used this approach to demonstrate that mitochondrial JNK signaling was a prominent event in the induction of dopaminergic neurodegeneration in adult rats exposed to 6-hydroxydopamine (Chambers et al., 2013). Collectively, these studies demonstrate that mitochondrial JNK signaling occurs in the brain.

Given the contributions of JNK to neurological function, our current study was designed to define the locations of mitochondrial JNK signaling in the adult brain in order to better understand how this signaling nexus contributes to physiological processes in the brain. We examined the abundance of Sab in different brain regions, its sub-neuronal localization and a putative role for Sab-mediated signaling in neuronal activity. Sab was found to be constitutively expressed throughout the adult mouse brain. Further, Sab was expressed in primary rat hippocampal cultures, cultured human astrocytes, and synaptosomes isolated from adult mice. Sab was found to be largely mitochondrial in axons, dendrites, and soma of hippocampal neurons. Inhibition of Sab-mediated signaling with the Tat-Sab_{KIM1} peptide impaired basal activity as indicated by decreased firing frequency and amplitude of spikes in cultured hippocampal neurons. Taken together, our studies demonstrate that Sab-mediated signaling is involved in normal neurological processes and the physiological role of JNK in the CNS may extend to the regulation of mitochondrial biology.

2. Results

2.1 Sab is expressed throughout the adult brain. To determine the potential distribution of mitochondrial JNK (or MAPK) signaling in the brain, we examined Sab mRNA levels in forty-nine (49) areas of the adult mouse brain (Figure 1A). Sab expression was widespread in the brain with particularly high levels in the hippocampus (CA1, CA2/CA3 and dentate gyrus), ventral midbrain (*substantia nigra* and ventral tegmental area) and cerebellum (vermis and lobe) (Figure 1A). We next dissected the brains of adult mice, and acquired proteins to examine the relative levels of Sab in distinct areas. Sab was detected in the olfactory bulb, frontal cortex, striatum, hippocampus, ventral midbrain, cerebellum, and brain stem (Figure 1B). In agreement with the RT-PCR data, Sab protein levels from six adult animals were abundant in the hippocampus, ventral midbrain, and cerebellum (Figure 1B and 1C).

2.2 Sab is expressed in neurons, at synapses, and in astrocytes. Given the brain distribution of Sab and the previously defined roles for JNK in neuronal function, we examined whether Sab was expressed in neurons, specifically at synapses. Cytosolic JNK activity is described as high in the hippocampus; therefore, we cultured hippocampal neurons (with less than 5% of glial cells) and assessed Sab expression by western blot analysis. Sab was found in cultured neurons (Figure 2A). The neuronal nature of these cells was confirmed by the presence of NeuN in Figure 2A. Since JNK has been implicated in synaptic transmission, we purified synaptosomes from adult rat brains. We determined the identity and relative contributions of distinct cellular compartments to our synaptosomal preparations by blotting for synapse proteins (PSD95, Synaptophysin, and NMDAR2B), mitochondrial markers (COX-IV and TOM20), cytosolic proteins (GAPDH and CaNA), nuclear marker (Histone H3) and a loading control (Actin). In Figure 2B, four (4) individual synaptosomal preparations show significant levels of Sab. Finally,

to evaluate if Sab was expressed in other cells within the brain, we assayed human fetal astrocytes for Sab expression and, as demonstrated in Figure 2C, Sab was expressed in astrocytes (Astrocytes were confirmed by the presence of GFAP – Figure 2C).

2.3 Hippocampal Sab is found in axons, dendrites, and synapses. Because cytosolic JNK activity is elevated in hippocampal neurons and Sab expression is particularly abundant in the hippocampus, we assessed the subcellular distribution of Sab using immunofluorescence and confocal microscopy in the CA1 hippocampal subfield. Sab presented the prototypic pattern of a mitochondrial protein, characterized by small intracellular puncta that were particularly apparent in the cell body of CA1 neurons and the major dendritic profiles of *stratum radiatum* (Figure 3A). To confirm the mitochondrial localization of Sab, we performed post-embedding electron microscopy and analyzed the distribution of gold particles in neuronal profiles of the adult mouse hippocampus. As shown in Figure 3, Sab labeling was selectively localized in mitochondria and was not associated with other cell organelles. Sab-positive mitochondria were observed in the different sub-neuronal compartments, *i.e.* cell bodies (Figure. 3B), dendrites (Figure 3C) and axon terminals (Figure 3D). Quantification of gold particle density in these compartments revealed a significant enrichment of Sab labeling in mitochondria compared with the surrounding cytoplasm (Table 1). To validate our microscopic localization of Sab to mitochondria, we dissected the hippocampal from eight-week-old male (n=4) and female (n=4) C57BL/6J mice. Mitochondria were isolated from hippocampal homogenates, and Western blot analysis was used to detect the presence of Sab in whole lysates, cytosol, and mitochondrial fractions (Figure 3E). Sab was found to be expressed in the whole lysate; however, minimal amounts of Sab were found in the cytosol, while Sab was enriched in the mitochondrial preparations (Figure 3E). To illustrate the enrichment and purity of our subfractions, we performed western blot analyses for

mitochondrial proteins TOM20 and COX-IV and the cytosolic marker GAPDH (Figure 3E). Calreticulin (CALR) and PEX19 were used to determine the relative levels of endoplasmic reticulum (ER) and peroxisome contamination, respectively. Histone H3 represented nuclear-based impurities (Figure 3E). To determine if the signal associated with Sab was specific and not due to antibody-related anomalies, we transduced rat pheochromocytoma PC-12 cells with lentiviruses carrying an empty pLenti6 vector or one encoding Sab with a 3xFLAG epitope on the C-terminus. Mitochondria were then isolated from PC-12 cells with the empty vector and vectors encoding Sab after five days of expression. Western blot analysis revealed that Sab, as in Figure 3E, was expressed in the PC-12 cells and resided primarily at mitochondria (Figure 3F). In the 3xFLAG-Sab encoding cells, a higher molecular weight band appeared, which was not present in the cells transduced with the empty vector (Figure 3F). A band cross-reactive with an FLAG-specific antibody was found at the same molecular weight as Sab and displayed the same subcellular localization as Sab at mitochondria; moreover, this higher molecular weight band was not found in the cells containing the empty vector (Figure 3F). As in the previous figure (Figure 3E), we confirmed our mitochondrial enrichment by evaluating COX-IV levels; meanwhile, the relative levels of cytosolic, ER, peroxisome, and nuclear contamination was observed by observing GAPDH, CALR, PEX19, and Histone H3 levels, respectively. Next, we employed confocal microscopy of the PC-12 cells transduced with lentivirus encoding 3xFLAG-Sab following fluorescent immunodetection of either Sab or the FLAG epitope. As seen in Figure 3G, the fluorescent signature of Sab (green) in the PC-12 cell overlaps with that of the signal from the anti-FLAG antibody (red). The colocalization can be observed by the yellow overlap of the anti-Sab and anti-FLAG fluorescence (Figure 3G, bottom right panel). Our data

demonstrate the specificity of the Sab antibody and confirm the mitochondrial localization of Sab in hippocampal neurons.

2.4 Inhibition of Sab-mediated signaling impairs spontaneous hippocampal neuron activity. To gain insight into the physiological role of Sab, we measured the spontaneous firing of cultured hippocampal neurons in high potassium using whole-cell patch clamping. Neurons were treated with either PBS, 5μM Tat-Scrambled peptide or 5μM Tat-Sab_{KIM1} (to inhibit Sab-mediated signaling) for 15 minutes before recording (Figure 4A). Untreated neurons or neurons treated with the Tat-Scramble peptide had similar spike rates and amplitudes (Figure 4A-C). Cultured hippocampal neurons treated with the Tat-Sab_{KIM1} peptide had a decreased firing frequency and spike amplitude, compared to untreated or scramble peptide-treated neurons (Figure 4B & 4C). To determine if the changes in neuronal activity were due to Sab-mediated events and not to putative nonspecific interactions of the Tat-Sab_{KIM1} peptide, we infected mouse primary hippocampal neurons at day 2 of in vitro culture (2 DIV) with lentiviruses harboring plasmids encoding shRNAs specific for Sab or a scrambled control. At 12 DIV, the cells were lysed, and the levels of Sab were determined using western blot analysis. Sab levels were markedly decreased (>70%) in neurons infected with viruses expressing the Sab shRNA, while neurons infected with the scramble control experience no significant change in Sab expression (Figure 4D top panel). The decrease in Sab occurred while the mitochondrial protein COX-IV demonstrated no change across conditions (Figure 4D, top panel). Actin was used as a loading control (Figure 4D, top panel). The abundance of Sab was determined by measuring the relative fluorescence of each band (Figure 4D, bottom panel); accordingly, Sab levels were lower in the cells infected with the lentivirus carrying the Sab shRNA (Figure 4D, bottom panel). Next, we normalized Sab expression to mitochondria abundance and uninfected cells, and we verified that

Sab protein levels had indeed decreased (Figure 4D, bottom panel). With Sab sufficiently knocked down, we were able to assess the effects of Sab-mediated events on neuronal activity. Neurons expressing the scrambled control shRNA were electrophysiologically comparable to untreated cells (Figure 4E); meanwhile, neurons expressing the Sab shRNA had decreased spike frequency (Figure 4E, left panel) and diminished spike amplitude (Figure 4E, right panel) compare to the neurons expressing the control shRNA. These reductions in spike rate, and amplitude were distinct from normal hippocampal neurons based on Mann-Whitney analysis ($P<0.05$). These results collectively demonstrate that Sab is expressed in neuronal mitochondria and that Sab-mediated signaling affects neuronal activity.

3. Discussion

MAPKs are crucial components of neuronal and cognitive functions, and elevated MAPK signaling is a common feature in neurological disease (Kim and Choi, 2010). Furthermore, mitochondrial MAPK signaling has emerged as a critical regulatory event for cellular and organelle physiology (Horbinski and Chu, 2005). In the current study, we examined the distribution of a MAPK mitochondrial scaffold protein, Sab and its contribution to neuronal function. Sab has been extensively linked to mitochondrial JNK signaling, which has been shown to induce mitochondrial dysfunction and cell death (Chambers et al., 2011a; Chambers and LoGrasso, 2011). Our examination of Sab expression in the brain revealed an enrichment of Sab in the hippocampus, ventral midbrain, and cerebellum (Figures 1A & 1B). Notably, Sab expression parallels that of JNK isoforms (JNK1, JNK2, & JNK3), the only known binding partners for Sab in the brain (Carboni et al., 1998). In particular, JNK3, the predominant brain isoform, has its highest activity in the hippocampus of adult mouse brains (Brecht et al., 2005; Carboni et al., 1998; Lein et al., 2007). Given the interaction between JNK and Sab and their

high expression, it is feasible to conceive that the JNK-Sab signaling nexus has a basic role in hippocampal physiology.

The regions identified in Figures 1A and 1B support neuronal processes related to learning and memory as well as motor control. Furthermore, Figure 2 demonstrates that Sab is expressed in synaptosomes, which reinforces a putative role for this signaling nexus in neurotransmission, especially, when one considers that Sab is found in axon terminals (Figure 2B and 3D). Additionally, the identification of significant Sab levels in astrocytes may indicate an important role for mitochondrial JNK signaling in other cells within the brain.

Previous research employed subcellular fractionation and fluorescent microscopy to determine that Sab is localized to mitochondria (Chambers et al., 2011a; Wiltshire et al., 2002; Win et al., 2011). For the first time, we used electron microscopy to determine the subcellular distribution of Sab. Gold particle labeling of Sab was found to be almost exclusively mitochondrial; intriguingly, Sab was not found to be associated with the ER (Figure 3B). The microscopic mitochondrial localization of Sab was verified using subcellular fractionation, which demonstrated a significant enrichment of Sab in mitochondrial preparations from adult mouse hippocampi (Figure 3E). We were able to confirm this localization using an epitope-tagged version of Sab that also colocalized with mitochondria (Figure 3F and 3G). The localization of Sab to mitochondria confirms the potential for this scaffold protein to sequester and concentrate MAPK signaling at mitochondria.

Labeling of Sab was present in mitochondria contained in distinct subcellular compartments, including dendritic profiles and axonal terminals (Figures 3B, 3C, and 3D). This is in agreement with the discovery of Sab in synaptosomes (Figures 2A & 2B). The presence of Sab in these subcellular compartments suggests that Sab may play a role in neurotransmission.

The distribution of Sab in neurons may polarize the activities of JNK isoforms with similar distributions. JNK3, the prevailing isoform in the hippocampus, appears to be largely relegated to the nucleus; in contrast, JNK1 is found predominantly in the cell body cytoplasm, axons, and dendrites (Coffey et al., 2002; Lee et al., 1999). This similar distribution of Sab and JNK1 may suggest a means by which JNK1 signaling could be enhanced on mitochondria through interaction with Sab. However, we cannot currently rule out that Sab may interact with other JNK isoforms or still undefined MAPKs on neuronal mitochondria.

At present, the precise function of Sab-mediated signaling in neurons is still unclear. One possibility is that Sab on the axonal mitochondria may be required for the expedited transport and recycling of depolarized mitochondria in energetic, demanding areas like dendrites and axon terminals. Mitochondria are essential to synaptic transmission, as these organelles provide ATP and calcium (Ivannikov et al., 2013). MAPKs, specifically JNK, have been shown to impact mitochondrial dynamics (Leboucher et al., 2012; Pyakurel et al., 2015). JNK has been shown to phosphorylate Mfn2 causing its degradation, which ultimately produced a fragmented mitochondrial network (Leboucher et al., 2012); likewise, ERK has been shown to act in a similar fashion with Mfn1 (Pyakurel et al., 2015). Sab could be the scaffold protein that facilitates these interactions. Thus, the Sab-MAPK interaction could be crucial in releasing mitochondria from the network in the cell body for use in axons and dendrites. One of the roles for JNK in the adult brain is the transport of macromolecular complexes to and from the synapse via an interaction with molecular motor proteins (Horiuchi et al., 2007; Verhey et al., 2001). One could also surmise that Sab is required to transport mitochondria to the synapse in a JNK-dependent manner. The roles of Sab-mediated signaling in axons and neurotransmission are under active investigation in our lab.

Based on the expression and broad distribution of Sab in the brain and the complementary distribution of cytosolic JNK activity, we reasoned that Sab-mediated signaling might have a role in basic neurophysiology. Herein, we report that inhibition of Sab-mediated signaling by the Tat-Sab_{KIM1} peptide significantly reduces the activity of cultured hippocampal neurons. In our electrophysiology experiments, inhibiting the Sab-JNK interaction caused a rapid reduction in neuronal activity. A similar effect has been noticed with JNK selective inhibitors *in vitro* and *in vivo* (Coffey, 2014; Yang et al., 2011); wherein, small molecule JNK inhibitors induced a decrease in basal synaptic transmission. We propose that the effects of the Tat-Sab_{KIM1} peptide are compatible with diminished basal activity caused by a loss of mitochondrial JNK activity; however, we cannot preclude that the Tat-Sab_{KIM1} peptide may be acting as a global JNK inhibitor (targeting both nuclear and mitochondrial signaling) in neurons. However, neurons expressing a Sab-specific shRNA also had reduced neuronal activity compared to controls (Figure 4E) further suggesting that Sab-mediated signaling events may be regulating fundamental aspects of neuronal physiology. Alternatively, it is possible that impairing neuronal Sab-mediated signaling could impair mitochondrial function or induce dysfunction that would lead to an inability to support neuronal firing resulting in the decreased spike rate and amplitude observed in our studies (Figure 4). Nonetheless, we suggest that Sab may be a novel platform for the regulation of synaptic transmission due to its distribution in the brain and neurons and its potential role in the spontaneous activity.

In this work, we have found that the mitochondrial MAPK scaffold protein Sab is well distributed throughout the adult brain. Sab expression overlaps with that of JNK isoforms in the hippocampus, ventral midbrain, and cerebellum. Sab is present in mitochondria and the neuronal in the cell body, axons, and dendrites, and is detected in synaptosomes suggesting that Sab-

mediated signaling is present in synapses; Furthermore, inhibition of Sab-mediated signaling impaired spontaneous firing of cultured hippocampal neurons. These data reinforce the importance of mitochondrial MAPK signaling in neurological function and disease. These studies represent a new perspective for MAPK signaling in the brain; wherein, regulation of subcellular MAPK signaling could be an essential factor in the balance of healthy cognitive function and neurodegenerative disease.

4. Materials and Methods

4.1 Ethical Standards and Animal Housing/Care: All experiments were approved by the institutional committees for animal care and utilization at Florida International University and the University of Torino; furthermore, studies were performed in accordance with the Society of Neuroscience and Italian guidelines. C57BL/6 mice (Jackson Laboratories, Bar Harbor, ME) were purchased at 4 weeks of age for studies conducted at FIU, while Sprague-Dawley rats (Harlan Laboratories, Indianapolis, IN) were purchased at 8 weeks of age. Mice were housed in sex-matched cages with no more than five (5) mice per cage, while rats were housed in pairs. Animals were allowed to feed ad libitum and were provided standard chow.

4.2 Sample acquisition and brain dissection: Mice and rats were euthanized and the brains were removed as described in our previous work. For RT-PCR analyses, brains from six (6) animals were sectioned into 0.5mm slices using a mouse brain matrix and frozen. For the microdissection of individual brain regions, specific slices were bilaterally punched with a 0.5mm diameter needle (Kasukawa et al., 2011). Two (2) slices were surveyed per animal for specific brain regions to assure replication within animals. For protein analysis, brains were dissected as previously described to isolate the olfactory bulb, frontal cortex, striatum, hippocampus, ventral midbrain, cerebellum, and brain stem (Spijker, 2011b). For a ventral midbrain isolate that was

devoid of hippocampus, cortex, cerebellum, and brain stem, we dissected the brain between -6.38 and -2.6 bregma. The brain stem was considered the region between the ventral midbrain and spinal cord minus the cerebellum; this section specifically contained the pons and medulla. The dissected regions of the brains were then homogenized in T-PER (Thermo-Fisher Scientific) supplemented with protease and phosphatase inhibitors. Homogenates were then analyzed by western blot analysis as described below. Human fetal astrocytes were purchased from ScienCell Research Laboratories (Carlsbad California), and cultured according to manufacturer's instructions. Astrocytes were lysed and analyzed by Western blot analysis according to our previously published protocol (Chambers et al., 2011f; Chambers et al., 2013).

4.3 RT-PCR detection of Sab: RNA was isolated from tissue punches using the Trizol reagent, and cDNA was synthesized using Superscript II-mediated reverse transcription from 0.4µg of total RNA. RT-PCR was performed in the ABI Prism 7500 instrument with SYBR Green reagents as previously described (Kasukawa et al., 2011). To determine the Sab levels across specific brain regions, we used a probe specific for a 130bp stretch near the 5'-end of the Sab ORF (5'-CGGAGCCGAAATCCTGCCG-3' and 5'-GACTGATTTAATTCTC-3'). RT-PCR results were normalized to both 18S rRNA and GAPDH levels in the brain. Data are presented in $\log_2$ format.

4.4 Primary hippocampal cultures: Mouse hippocampal neurons purchased from Gibco Life Technologies (A15587, Invitrogen, Carlsbad, CA) were plated in plastic 6-well plates, previously coated with 0.1 mg/mL of poly-L-lysine. The plating density was $1.6x10^5$ cells/well. Neurons were grown for fourteen (14) days in Neurobasal medium supplemented with 2% B27 and 0.5 mM L-glutamine, at 37°C and 5% CO_2.

4.5 Purification of synaptosomes: Synaptosomes were purified from Sprague-Dawley rat brains (excluding the cerebellum) as previously described elsewhere (Sodero et al, 2012)(Pilo Boyl et al., 2007). Rats were used to provide a larger preparation of synaptosomes in the event mitochondria needed to be purified for western blot analysis. Briefly, the brains were quickly removed, the olfactory bulb and cerebellum were dissected out, and the tissue was homogenized in ice-cold buffer (320 mM sucrose, 1 mM EDTA and 5 mM HEPES; pH 7.4). The homogenization consisted of eight strokes in a glass-Teflon homogenizer. The homogenate was spun at 3,000xg for 10 minutes. Then, the supernatant was spun at 14,000xg for 10 minutes. The pelleted crude synaptosomes were suspended in Kreb's-Ringer buffer (140 mM NaCl, 5 mM KCl, 5 mM glucose, 1 mM EDTA and 10 mM HEPES; pH 7.4) and mixed with Percoll to reach a final Percoll concentration of 45%. The samples were spun at 18,000xg for 2 minutes and the synaptosomes were recovered from the top of the Percoll suspension. Finally, the synaptosomes were washed in Kreb's-Ringer buffer by spinning them at 18000xg for 30 seconds. The quality of each synaptosome preparation was determined using Western blot analysis of distinct compartments. Brain homogenates, cytosolic supernatants, and synaptosomes were probed for the levels of Sab, ubiquitous markers GAPDH and Actin, nuclear protein Histone H3, cytosolic protein, Calcineurin (CaNA), synaptosomal markers (post-synaptic density protein 95 (PSD95), synaptophysin, and N-methyl-D-aspartate receptor 2B (NMDAR2B)), and mitochondrial proteins cyclo-oxygenase IV (COX-IV) and translocase of the outer membrane 20 (TOM20).

4.6 Lysis and Immunoblotting: Cultured neurons were washed 2 times with ice-cold PBS and then harvested in Radioimmunoprecipitation Assay (RIPA) buffer (50mM Tris-HCl, 150mM NaCl, 1% NP-40, 0.5% sodium deoxycholate and 0.1% sodium dodecyl sulfate, 5mM EDTA and 1mM EGTA; pH 7.4) containing HALT® protease inhibitor and phosphatase inhibitor cocktails

(Thermo Scientific, Waltham, MA). The lysate was cleared by centrifugation at 12,000 RPM for 10 minutes. Purified synaptosomes and brain regions were also lysed in RIPA buffer. The protein concentration of the different lysates was assessed in triplicates using the BCA Protein Assay (Pierce Biotechnology, Rockford, IL). Equivalent amounts of total protein were separated by SDS-PAGE and then transferred to nitrocellulose membranes. The membranes were blocked with 3% BSA in TBS containing 0.1% (v/v) Tween-20 at room temperature for 1 hour, and then probed overnight with mouse monoclonal anti-Sab (1/1,000; Novus Biologicals #H00009467-M01) and rabbit monoclonal anti GAPDH (1/5,000; Cell Signaling Technology #5174), NeuN (1/1,000; Cell Signaling Technology #24307), COX-IV (1/2,000; Cell Signaling Technology #11967), Calcineurin (CaNA; 1/1,1000 Cell Signaling Technology #2614), TOM20 (1,1000; Cell Signaling Technology #42406), PSD95 (1,1000; Cell Signaling Technology #3450), Synaptophysin (1/1,000; Cell Signaling Technology #5461), NMDAR2B (1/1,000 Cell Signaling Technology #14544), Histone H3 (1/1,000 Cell Signaling Technology #4499), GFAP (1/1,000; Cell Signaling Technology #12389), and Actin (1/10,000; Cell Signaling Technology #4970). The membranes were then incubated with appropriate fluorescent secondary antibodies (1/20,000; DyLight Anti-mouse 800 and Anti-rabbit 680, Cell Signaling Technologies, #5257 and #5366) for 1 hour at room temperature, and finally scanned using a Li-Cor Biosciences Odyssey CLx device. Images were quantified with the Image J 1.48v software (NIH, USA).

4.7 Confocal microscopy and immunofluorescence: Anesthetized mice were perfused with Ringer's solution followed by 1% formaldehyde in 0.1 M phosphate buffer (PB). The brain was dissected and cut with a vibratome (100 µm). Free-floating hippocampal sections were pre-incubated in 0.02 M PBS containing 5% normal goat serum (PBS–5% NGS) for 30 min, and then incubated overnight in mouse monoclonal anti-Sab diluted 1/500. Sections were then

incubated for 1 hour in Alexa Fluor 488 anti-mouse IgG secondary antibodies (1/500), washed in PBS and mounted in Vectashield (Vector Laboratories) (Pilo Boyl et al., 2007). Routine immunocytochemical controls included the omission of the primary antibody. Images were acquired using a Zeiss Pascal confocal laser scanning microscope.

For PC-12 cells, cells were grown on 18 x 18-mm poly-D-lysine coated German glass coverslips at a density of 2.0 x 10^5 cells/well in a six-well plate. Cells were grown to ~75% confluency and then fixed in 4% paraformaldehyde for 25 minutes at room temperature. The cells/coverslips were washed twice in PBS and then quenched in 100 mM glycine for 20 minutes. The cells were next permeabilized in PBS containing 0.1% Triton X-100. The cells were blocked at room temperature for one hour in PBS with 0.0s% Triton and 5% BSA. The samples were incubated with primary antibodies for Sab (1:500) and FLAG (1:250) for 2.5 hours at room temperature. The cells were washed with PBS followed by an incubation with donkey anti-mouse AlexaFluor488 and goat anti-rabbit AlexaFluor566 at room temperature for 1.5 hours. After the incubation with the secondary antibodies, the samples were washed with PBS, and coverslips were mounted using Vectasheild with DAPI. Fluorescent microscopy was conducted on the Olympus FV1200 laser scanning confocal microscope under the 60X oil objective. The exposure for each channel was: FITC, 0.62ms, TRITC, 0.81ms. The gain was set to 3.7. Six images were taken per biological replicate to assure the observations were consistent among transductions.

4.8 Post-embedding electron microscopy: Hippocampal sections were obtained from tissue blocks that had been freeze-substituted with methanol and embedded in Lowicryl HM20 for a previous study (Pilo Boyl et al., 2007). Postembedding immunogold labeling was performed on ultrathin sections using goat anti-mouse secondary antibodies coupled to 10 nm colloidal gold particles (British BioCell International, Cardiff, UK). All procedures have been described in

detail in Sassoè-Pognetto and Ottersen (2000). The grids were observed with a JEM-1010 transmission electron microscope (Jeol, Japan) equipped with a side-mounted CCD camera (Mega View III, Olympus Soft Imaging System, Germany). Gold labeling was quantified in randomly selected grid squares in CA1 *stratum pyramidale* (cell bodies) and *stratum radiatum* (dendrites and axon terminals) in sections from three mice (Sassoè-Pognetto and Ottersen, 2000). The area of profiles was measured using the Image J software.

4.9 Mitochondrial Enrichment: Hippocampi from eight-week-old adult C57BL/6J mice (Jackson Labs) were acquired as described above in subsection 4.2 according to established protocols (Brewer and Torricelli, 2007; Spijker, 2011a). To account for potential differences between sexes four male and four female mice were used for the study. PC-12 cells (ATCC CRL-1721) were cultured in RPMI-1640 supplemented with 10% heat-inactivated horse serum and 5% heat-inactivated fetal bovine serum under normal cell culture conditions (37^{o}C, 5% CO_2, and humidity). Mitochondria were isolated from dissected hippocampi and PC-12 cells using approaches described in our previous work (Chambers et al., 2011a; Chambers et al., 2013). For hippocampal mitochondrial isolates, the entire hippocampus from each animal was placed in 1mL homgenization buffer (225mM mannitol, 75mM sucrose, 5mM HEPES (pH 7.4), 1mM EGTA and 2% fatty-acid free BSA) and homogenized in a Dounce homogenizer for 30 strokes (Chinopoulos et al., 2011). The homogenate was cleared by centrifugation at 500xg (5 minutes at 4^{o}C); the supernatant was then centrifuged at 14,000xg for 10 minutes at 4^{o}C. The pellet was resuspending in 12% Percoll^{TM} (in homogenization buffer) and layered with 24% Percoll^{TM} (in homogenization buffer) before centrifuging again at 18,000xg at 4^{o}C for 15minutes. For PC-12 cells, we used our protocol described in (Chambers and LoGrasso, 2011)The crude mitochondrial pellet was suspended in 35% Histodenz (in homogenization buffer), layered with

40%, 25%, and 15% Histodenz solutions, and centrifuged at 4°C for 90 minutes at 52,000xg to minimize contamination of ER and peroxisomes (Graham, 2001). The mitochondria were extracted from the 25/35% interface and resuspended in RIPA lysis buffer for protein analysis. The level of mitochondrial protein was quantified using microplate BCA analysis, and the purity of the mitochondrial preps was determined by western blot analysis for mitochondrial proteins TOM20 and COX-IV, while cytosolic, ER, nuclear, and peroxisomal contamination was determined by Western blotting for GAPDH, calreticulin (CALR), histone H3, and PEX19, respectively. Only enrichments containing mitochondria of greater tan 80% purity were used for our analysis.

4.10 Manipulation of Sab Expression: To determine if the Sab antibody was specific, we ectopically expressed Sab using lentiviral transduction in PC-12 cells. The Sab ORF was cloned into the pLenti6-3xFLAG plasmid (Invitrogen) to append a C-terminal 3xFLAG epitope to Sab since the C-terminal epitope would not interfere with translocation to mitochondria. Briefly, lentiviral particles were produced using human HEK-293T cells according to manufacturer's ViraPower™ Lentiviral Packaging Kit instructions. Viral titers were determined using a near-infrared ELISA approach (Chambers et al., 2017) that recognizes viral p24 protein similar to the protocol employed by (Weldon et al., 2010). PC-12 cells seeded in three 150-mm plates were then infected with an MOI of 4 and cells were lysed after five days of infection and mitochondrial isolates were made as described above.

To evaluate if the neuronal effects of the Tat-Sab_{KIM1} peptide were Sab-mediated events, we silenced Sab in primary hippocampal neurons using lentiviral introduction of plasmids (pGIPZ – Thermo Scientific) encoding either a Sab-specific shRNA or a scrambled control shRNA. Viral titers were determined using the $TCID_{50}$ approach, which evaluates the number of cells infected

with a GFP-expressing virus (Chambers et al., 2010). Primary hippocampal neurons were then infected with the lentivirus at a minimal MOI of 15 in the presence of 6μg/mL polybrene at two days of *in vitro* culture (DIV). Protein levels were examined at 12 DIV using western blot analysis. To quantitatively determine the relative changes in Sab protein levels, we measured the fluorescence intensity (using the median background subtraction setting) of bands on Western blots corresponding to Sab using the Li-Cor Odyssey CLx imager and the accompanying Image Studio Software. To normalize the data to mitochondria protein levels, we divided the fluorescent intensity of Sab bands by the COX-IV band fluorescent intensity on each membrane. We then divided each of the treatments by the mock controls to normalize the measures to the "untreated" neurons for each experiment. Electrophysiology experiments (described below) were conducted at 14 DIV, which was twelve days following the introduction of the silencing constructs.

4.11 Electrophysiology: Whole-cell patch clamp recordings were performed on pairs of synaptically-linked cultured hippocampal neurons grown on coverslips for 14 days (Balena et al., 2008; Hamill et al., 1981). The neurons were placed in artificial cerebrospinal fluid (ACSF – 130mM NaCl, 2.5mM KCl, 15mM HEPES, 1.3mM NaH_2PO_4, 10mM glucose, 2mM $CaCl_2$, and 2mM $MgSO_4$, pH 7.4) and adapted for 30 minutes. The cells were then transferred to a recording solution containing 145mM NaCl, 2.5mM KCl, 2mM $CaCl_2$, 1mM $MgCl_2$, and 10mM HEPES, pH 7.4. For high potassium experiments with concentration of KCl was increased to 25mM. The recording pipettes were pulled from glass capillaries with a resistance of 4-10MΩ, and the pipette was filled with a solution of 135mM K-gluconate, 2mM $MgCl_2$, 10mM HEPES, 7mM NaCl, and 2mM Na_2ATP, pH 7.2 with an osmolarity of 270mOsm. Signals were recorded using

an AxoPatch 200B amplifier with 2-kHz filter (Molecular Devices). Data were transferred from the pCLAMP 10 software (Molecular Devices) to GraphPad Prism 6.0 for analysis.

To determine the effect of Sab-mediated signaling on spontaneous firing, primary hippocampal neurons adapting in ACSF were treated with either PBS, 5µM Tat-Sab_{KIM1} or the Tat-Scramble control for the final 15 minutes of acclimation. Neurons were then placed in the extracellular solution mentioned above containing the same concentrations of peptide. To induce spontaneous firing, the potassium concentration in the solution was increased to 25mM. Signals were recorded for 30 seconds following the addition of potassium.

4.12 Statistical analysis and replicates: Data were analyzed using one-sided analysis of variance (ANOVA) and Mann-Whitney tests. For all studies a minimum of three biological replicates or three animals were required.

5. Acknowledgements

The authors would like to acknowledge the assistance of Ms. Gabriela Goldberg and Iru Paudel for their helpful comments during the preparation, editing, and revising of the manuscript.

6. Funding

This work has been supported by a generous start-up fund provided by the Herbert Wertheim College of Medicine and Florida International University to JWC. M.R.S was supported by NIH/NIGMS R25 GM06134. This research did not receive any specific grant from funding agencies in the public, commercial, or not-for-profit sectors.

7. References

Aoki, H., Kang, P.M., Hampe, J., Yoshimura, K., Noma, T., Matsuzaki, M., Izumo, S., 2002. Direct activation of mitochondrial apoptosis machinery by c-Jun N-terminal kinase in adult cardiac myocytes. J Biol Chem. 277**,** 10244-50.

Balena, T., Acton, B.A., Koval, D., Woodin, M.A., 2008. Extracellular potassium regulates the chloride reversal potential in cultured hippocampal neurons. Brain Research. 1205**,** 12-20.

Bjorkblom, B., Ostman, N., Hongisto, V., Komarovski, V., Filen, J.J., Nyman, T.A., Kallunki, T., Courtney, M.J., Coffey, E.T., 2005. Constitutively active cytoplasmic c-Jun N-terminal kinase 1 is a dominant regulator of dendritic architecture: role of microtubule-associated protein 2 as an effector. J Neurosci. 25**,** 6350-61.

Brecht, S., Kirchhof, R., Chromik, A., Willesen, M., Nicolaus, T., Raivich, G., Wessig, J., Waetzig, V., Goetz, M., Claussen, M., Pearse, D., Kuan, C.Y., Vaudano, E., Behrens, A., Wagner, E., Flavell, R.A., Davis, R.J., Herdegen, T., 2005. Specific pathophysiological functions of JNK isoforms in the brain. Eur J Neurosci. 21**,** 363-77.

Brewer, G.J., Torricelli, J.R., 2007. Isolation and culture of adult neurons and neurospheres. Nat. Protocols. 2**,** 1490-1498.

Carboni, L., Carletti, R., Tacconi, S., Corti, C., Ferraguti, F., 1998. Differential expression of SAPK isoforms in the rat brain. An in situ hybridisation study in the adult rat brain and during post-natal development. Brain Res Mol Brain Res. 60**,** 57-68.

Cavalli, V., Kujala, P., Klumperman, J., Goldstein, L.S., 2005. Sunday Driver links axonal transport to damage signaling. J Cell Biol. 168**,** 775-87.

Chambers, J.W., Maguire, T.G., Alwine, J.C., 2010. Glutamine metabolism is essential for human cytomegalovirus infection. J Virol. 84**,** 1867-73.

Chambers, J.W., Cherry, L., Laughlin, J.D., Figuera-Losada, M., Lograsso, P.V., 2011a. Selective inhibition of mitochondrial JNK signaling achieved using peptide mimicry of the Sab kinase interacting motif-1 (KIM1). ACS Chem Biol. 6**,** 808-18.

Chambers, J.W., LoGrasso, P.V., 2011. Mitochondrial c-Jun N-terminal kinase (JNK) signaling initiates physiological changes resulting in amplification of reactive oxygen species generation. J Biol Chem. 286**,** 16052-62.

Chambers, J.W., Pachori, A., Howard, S., Ganno, M., Hansen, D., Jr., Kamenecka, T., Song, X., Duckett, D., Chen, W., Ling, Y.Y., Cherry, L., Cameron, M.D., Lin, L., Ruiz, C.H., Lograsso, P., 2011f. Small Molecule c-jun-N-terminal Kinase (JNK) Inhibitors Protect Dopaminergic Neurons in a Model of Parkinson's Disease. ACS Chem Neurosci. 2**,** 198-206.

Chambers, J.W., Howard, S., LoGrasso, P.V., 2013. Blocking c-Jun N-terminal kinase (JNK) translocation to the mitochondria prevents 6-hydroxydopamine-induced toxicity in vitro and in vivo. J Biol Chem. 288**,** 1079-87.

Chambers, T.P., Santiesteban, L., Gomez, D., Chambers, J.W., 2017. Sab mediates mitochondrial dysfunction involved in imatinib mesylate-induced cardiotoxicity. Toxicology. 382**,** 24-35.

Chen, J.T., Lu, D.H., Chia, C.P., Ruan, D.Y., Sabapathy, K., Xiao, Z.C., 2005. Impaired long-term potentiation in c-Jun N-terminal kinase 2-deficient mice. J Neurochem. 93**,** 463-73.

Chinopoulos, C., Zhang, S.F., Thomas, B., Ten, V., Starkov, A.A., 2011. Isolation and Functional Assessment of Mitochondria from Small Amounts of Mouse Brain Tissue. In Neurodegeneration: Methods and Protocols. Vol., G. Manfredi, H. Kawamata, ed.^eds. Humana Press, Totowa, NJ, pp. 311-324.

Coffey, E.T., Hongisto, V., Dickens, M., Davis, R.J., Courtney, M.J., 2000. Dual roles for c-Jun N-terminal kinase in developmental and stress responses in cerebellar granule neurons. J Neurosci. 20**,** 7602-13.

Coffey, E.T., Smiciene, G., Hongisto, V., Cao, J., Brecht, S., Herdegen, T., Courtney, M.J., 2002. c-Jun N-terminal protein kinase (JNK) 2/3 is specifically activated by stress, mediating c-Jun activation, in the presence of constitutive JNK1 activity in cerebellar neurons. J Neurosci. 22**,** 4335-45.

Coffey, E.T., 2014. Nuclear and cytosolic JNK signalling in neurons. Nat Rev Neurosci. 15**,** 285-99.

Feltrin, D., Fusco, L., Witte, H., Moretti, F., Martin, K., Letzelter, M., Fluri, E., Scheiffele, P., Pertz, O., 2012. Growth cone MKK7 mRNA targeting regulates MAP1b-dependent microtubule bundling to control neurite elongation. PLoS Biol. 10**,** e1001439.

Graham, J.M., 2001. Isolation of Mitochondria from Tissues and Cells by Differential Centrifugation. In Current Protocols in Cell Biology. Vol., ed.^eds. John Wiley & Sons, Inc.

Gupta, S., Barrett, T., Whitmarsh, A., Cavanagh, J., Sluss, H., Derijard, B., Davis, R., 1996. Selective interaction of JNK protein kinase isoforms with transcription factors. EMBO J. 15**,** 2760 - 2770.

Hamill, O.P., Marty, A., Neher, E., Sakmann, B., Sigworth, F.J., 1981. Improved patch-clamp techniques for high-resolution current recording from cells and cell-free membrane patches. Pflügers Archiv. 391**,** 85-100.

Harris, C.A., Johnson, E.M., Jr., 2001. BH3-only Bcl-2 family members are coordinately regulated by the JNK pathway and require Bax to induce apoptosis in neurons. J Biol Chem. 276**,** 37754-60.

Horbinski, C., Chu, C.T., 2005. Kinase signaling cascades in the mitochondrion: a matter of life or death. Free Radical Biology and Medicine. 38**,** 2-11.

Horiuchi, D., Collins, C., Bhat, P., Barkus, R., Diantonio, A., Saxton, W., 2007. Control of a kinesin-cargo linkage mechanism by JNK pathway kinases. Curr Biol. 17**,** 1313 - 1317.

Hu, Y., Metzler, B., Xu, Q., 1997. Discordant activation of stress-activated protein kinases or c-Jun NH2-terminal protein kinases in tissues of heat-stressed mice. J Biol Chem. 272**,** 9113-9.

Ivannikov, M., Sugimori, M., Llinás, R., 2013. Synaptic Vesicle Exocytosis in Hippocampal Synaptosomes Correlates Directly with Total Mitochondrial Volume. Journal of Molecular Neuroscience. 49**,** 223-230.

Kasukawa, T., Masumoto, K.H., Nikaido, I., Nagano, M., Uno, K.D., Tsujino, K., Hanashima, C., Shigeyoshi, Y., Ueda, H.R., 2011. Quantitative expression profile of distinct functional regions in the adult mouse brain. PLoS One. 6**,** e23228.

Kim, E.K., Choi, E.-J., 2010. Pathological roles of MAPK signaling pathways in human diseases. Biochimica et Biophysica Acta (BBA) - Molecular Basis of Disease. 1802**,** 396-405.

Knott, A.B., Perkins, G., Schwarzenbacher, R., Bossy-Wetzel, E., 2008. Mitochondrial fragmentation in neurodegeneration. Nat Rev Neurosci. 9**,** 505-18.

Leboucher, Guillaume P., Tsai, Yien C., Yang, M., Shaw, Kristin C., Zhou, M., Veenstra, Timothy D., Glickman, Michael H., Weissman, Allan M., 2012. Stress-Induced Phosphorylation and Proteasomal Degradation of Mitofusin 2 Facilitates Mitochondrial Fragmentation and Apoptosis. Molecular Cell. 47**,** 547-557.

Lee, J.K., Park, J., Lee, Y.D., Lee, S.H., Han, P.L., 1999. Distinct localization of SAPK isoforms in neurons of adult mouse brain implies multiple signaling modes of SAPK pathway. Brain Res Mol Brain Res. 70**,** 116-24.

Lei, K., Davis, R.J., 2003. JNK phosphorylation of Bim-related members of the Bcl2 family induces Bax-dependent apoptosis. Proc Natl Acad Sci U S A. 100**,** 2432-7.

Lein, E.S., Hawrylycz, M.J., Ao, N., Ayres, M., Bensinger, A., Bernard, A., Boe, A.F., Boguski, M.S., Brockway, K.S., Byrnes, E.J., Chen, L., Chen, L., Chen, T.M., Chin, M.C., Chong, J., Crook, B.E., Czaplinska, A., Dang, C.N., Datta, S., Dee, N.R., Desaki, A.L., Desta, T., Diep, E., Dolbeare, T.A., Donelan, M.J., Dong, H.W., Dougherty, J.G., Duncan, B.J., Ebbert, A.J., Eichele, G., Estin, L.K., Faber, C., Facer, B.A., Fields, R., Fischer, S.R., Fliss, T.P., Frensley, C., Gates, S.N., Glattfelder, K.J., Halverson, K.R., Hart, M.R., Hohmann, J.G., Howell, M.P., Jeung, D.P., Johnson, R.A., Karr, P.T., Kawal, R., Kidney, J.M., Knapik, R.H., Kuan, C.L., Lake, J.H., Laramee, A.R., Larsen, K.D., Lau, C., Lemon, T.A., Liang, A.J., Liu, Y., Luong, L.T., Michaels, J., Morgan, J.J., Morgan, R.J., Mortrud, M.T., Mosqueda, N.F., Ng, L.L., Ng, R., Orta, G.J., Overly, C.C., Pak, T.H., Parry, S.E., Pathak, S.D., Pearson, O.C., Puchalski, R.B., Riley, Z.L., Rockett, H.R., Rowland, S.A., Royall, J.J., Ruiz, M.J., Sarno, N.R., Schaffnit, K., Shapovalova, N.V., Sivisay, T., Slaughterbeck, C.R., Smith, S.C., Smith, K.A., Smith, B.I., Sodt, A.J., Stewart, N.N., Stumpf, K.R., Sunkin, S.M., Sutram, M., Tam, A., Teemer, C.D., Thaller, C., Thompson, C.L., Varnam, L.R., Visel, A., Whitlock, R.M., Wohnoutka, P.E., Wolkey, C.K., Wong, V.Y., Wood, M., Yaylaoglu, M.B., Young, R.C., Youngstrom, B.L., Yuan, X.F., Zhang, B., Zwingman, T.A., Jones, A.R., 2007. Genome-wide atlas of gene expression in the adult mouse brain. Nature. 445**,** 168-76.

Li, X.M., Li, C.C., Yu, S.S., Chen, J.T., Sabapathy, K., Ruan, D.Y., 2007. JNK1 contributes to metabotropic glutamate receptor-dependent long-term depression and short-term synaptic plasticity in the mice area hippocampal CA1. Eur J Neurosci. 25**,** 391-6.

Lin, M.T., Beal, M.F., 2006. Mitochondrial dysfunction and oxidative stress in neurodegenerative diseases. Nature. 443**,** 787-95.

Lundby, A., Secher, A., Lage, K., Nordsborg, N.B., Dmytriyev, A., Lundby, C., Olsen, J.V., 2012. Quantitative maps of protein phosphorylation sites across 14 different rat organs and tissues. Nat Commun. 3**,** 876.

Pilo Boyl, P., Di Nardo, A., Mulle, C., Sassoè-Pognetto, M., Panzanelli, P., Mele, A., Kneussel, M., Costantini, V., Perlas, E., Massimi, M., Vara, H., Giustetto, M., Witke, W., 2007. Profilin2 contributes to synaptic vesicle exocytosis, neuronal excitability, and novelty-seeking behavior. The EMBO Journal. 26**,** 2991-3002.

Putcha, G.V., Moulder, K.L., Golden, J.P., Bouillet, P., Adams, J.A., Strasser, A., Johnson, E.M., 2001. Induction of BIM, a proapoptotic BH3-only BCL-2 family member, is critical for neuronal apoptosis. Neuron. 29**,** 615-28.

Putcha, G.V., Le, S., Frank, S., Besirli, C.G., Clark, K., Chu, B., Alix, S., Youle, R.J., LaMarche, A., Maroney, A.C., Johnson, E.M., Jr., 2003. JNK-mediated BIM phosphorylation potentiates BAX-dependent apoptosis. Neuron. 38**,** 899-914.

Pyakurel, A., Savoia, C., Hess, D., Scorrano, L., 2015. Extracellular Regulated Kinase Phosphorylates Mitofusin 1 to Control Mitochondrial Morphology and Apoptosis. Molecular Cell. 58**,** 244-254.

Sassoè-Pognetto, M., Ottersen, O.P., 2000. Organization of Ionotropic Glutamate Receptors at Dendrodendritic Synapses in the Rat Olfactory Bulb. The Journal of Neuroscience. 20**,** 2192-2201.

Small, S.A., Schobel, S.A., Buxton, R.B., Witter, M.P., Barnes, C.A., 2011. A pathophysiological framework of hippocampal dysfunction in ageing and disease. Nat Rev Neurosci. 12**,** 585-601.

Spijker, S., 2011a. Dissection of Rodent Brain Regions. In T Neuroproteomics. Neuromethods, Vol. 57, ed.^eds., pp. 13-26.

Spijker, S., 2011b. Dissection of Rodent Brain Regions. In Neuroproteomics. Vol., W.K. Li, ed.^eds. Humana Press, Totowa, NJ, pp. 13-26.

Tararuk, T., Ostman, N., Li, W., Bjorkblom, B., Padzik, A., Zdrojewska, J., Hongisto, V., Herdegen, T., Konopka, W., Courtney, M.J., Coffey, E.T., 2006. JNK1 phosphorylation of SCG10 determines microtubule dynamics and axodendritic length. J Cell Biol. 173**,** 265-77.

Verhey, K.J., Meyer, D., Deehan, R., Blenis, J., Schnapp, B.J., Rapoport, T.A., Margolis, B., 2001. Cargo of kinesin identified as JIP scaffolding proteins and associated signaling molecules. J Cell Biol. 152**,** 959-70.

Weldon, S.K., Mischnick, S.L., Urlacher, T.M., Ambroz, K.L.H., 2010. Quantitation of virus using laser-based scanning of near-infrared fluorophores replaces manual plate reading in a virus titration assay. Journal of Virological Methods. 168**,** 57-62.

Wiltshire, C., Matsushita, M., Tsukada, S., Gillespie, D.A., May, G.H., 2002. A new c-Jun N-terminal kinase (JNK)-interacting protein, Sab (SH3BP5), associates with mitochondria. Biochem J. 367**,** 577-85.

Wiltshire, C., Gillespie, D.A., May, G.H., 2004. Sab (SH3BP5), a novel mitochondria-localized JNK-interacting protein. Biochem Soc Trans. 32**,** 1075-7.

Win, S., Than, T.A., Han, D., Petrovic, L.M., Kaplowitz, N., 2011. c-Jun N-terminal kinase (JNK)-dependent acute liver injury from acetaminophen or tumor necrosis factor (TNF) requires mitochondrial Sab protein expression in mice. J Biol Chem. 286**,** 35071-8.

Win, S., Than, T.A., Fernandez-Checa, J.C., Kaplowitz, N., 2014. JNK interaction with Sab mediates ER stress induced inhibition of mitochondrial respiration and cell death. Cell Death Dis. 5**,** e989.

Yang, H., Courtney, M.J., Martinsson, P., Manahan-Vaughan, D., 2011. Hippocampal long-term depression is enhanced, depotentiation is inhibited and long-term potentiation is unaffected by the application of a selective c-Jun N-terminal kinase inhibitor to freely behaving rats. Eur J Neurosci. 33**,** 1647-55.

8. Figure Legends

Figure 1. Sab is differentially expressed in the adult rodent brain. RT-PCR was conducted to measure the expression levels of Sab in 49 areas of the adult mouse brain. Areas of increased Sab expression are marked as Hippocampus, VTA & SNpc, and Cerebellum (A). A representative western blot analysis of a dissected adult mouse brain showing the expression of Sab in different regions of the mouse brain (B). The relative Sab fluorescence was normalized to actin levels in each region. The average relative Sab expression from six (6) mice is presented for the western images and individual animal expression levels are illustrated as open circles on each column. (C).

Figure 2. Sab is expressed in neurons, at synapses, and in astrocytes. Western blot analysis for Sab expression in primary hippocampal cultures (indicated by the presence of NeuN) was

performed (A). Sab in rat synaptosomes was measured by western blot (B). The enrichment of synapses was confirmed by the increased levels of synaptic proteins PSD96, Synaptophysin, and NMDAR2B. The relative contributions of other compartments was determine by the levels of cytosolic proteins (GAPDH and CaNA), mitochondrial markers (COX-IV and TOM20), and nuclear protein, Histone H3. Actin was used as a loading control. Sab levels were also monitored by western blot in human fetal astrocytes (as indicated by the presence of GFAP) (C). COX-IV was used as a mitochondrial abundance control and GADPH was used as loading control in both A and C.

Figure 3. Sab localizes to mitochondria in hippocampal neurons. Sab immunoreactivity is concentrated in mitochondria. A. Confocal image through the hippocampal CA1. Immunolabeling for Sab is characterized by small puncta in the cell body and dendrites of hippocampal neurons. So: *stratum oriens*; Sp: *stratum pyramidale*; Sr: *stratum radiatum*. B. Electron micrograph showing immunogold labeling for Sab in the cell body of a pyramidal neuron. Gold particles decorate mitochondria (Mito), whereas the nucleus (Nu), Golgi complex (Go) and endoplasmic reticulum (Er) are unlabeled. C. Strong mitochondrial labeling for Sab in a dendritic profile in *stratum radiatum*. D. Axo-spinous synapse in *stratum radiatum*; note the strong immunogold labeling for Sab in two mitochondria within the presynaptic axon terminal (Ax). Sp: dendritic spine. Scale bars: A = 10 mm; B = 250 nm (applies to B-D). E. Mitochondria were isolated from the hippocampi of adult (8-week-old) male (n=4) and female (n=4) C57BL/6J mice and analyzed for the presence of Sab. Mitochondrial enrichment was determined by the relative abundance of TOM20 and COX-IV, while contamination by the cytosol (GAPDH), ER (CALR), peroxisomes (PEX19), and nucleus (Histone H3) was determined. The results from one representative animal is shown. F. PC-12 cells were infected with lentivirus (MOI = 4) for five days before isolating mitochondria from cells containing and empty vector (pLenti) or a vector expressing a C-terminal epitope-tagged Sab (pLenti:Sab3xFLAG). Immunoblots were used to determine the distribution of Sab. Mitochondrial enrichment and purity were assessed as described in the preceding panel. G. Confocal

microscopy of immunofluorescent labeling of epitope-tagged Sab (3xFLAG-Sab) was performed to validate the colocalization of Sab and the epitope. Here a representative PC-12 cell has been labeled with antibodies specific for Sab (top left) and FLAG (top right). A phase image is shown of the cell (bottom left) as well as a merged image of Sab and FLAG immunoreactivity (bottom right).

Figure 4. Inhibition of Sab-mediated signaling decreases basal firing frequency and amplitude. Whole-cell patch clamp was performed on cultured hippocampal neurons were with either PBS (untreated), 5μM Tat-Scramble, or 5μM Tat-Sab_{KIM1} for 15 minutes before high potassium treatment and recordings. Representative recordings for each treatment group are shown in A. The spike frequency (B) and amplitude (C) was determined over 20 seconds for each record for a minimum of four (4) cultures. Each experiment is represented with an open circle on each box and whisker plot (B & C). D. (top panel) Primary mouse hippocampal neurons were transduced with lentiviruses (MOI =15) expressing either a scramble shRNA control or a Sab-specific shRNA (Sab shRNA) at 2 DIV. At 12 DIV the cells were lysed, and Sab levels were assessed by western blot analysis. Actin was used as a loading control, while COX-IV was used as an index for mitochondrial abundance. (bottom panel) Sab protein levels were assessed by measuring the relative fluorescent intensity of each band, and the relative abundance of Sab was then normalized to COX-IV fluorescence and the intensity of Sab fluorescence in mock-infected neurons for six individual cultures of each condition (mock – n=6, Scrambled shRNA – n=6, and Sab shRNA – n=6). E. At 14 DIV (12 days after infection), primary hippocampal neurons were surveyed for neuronal activity as described for panels B and C. Statistical differences between conditions were determined using a Mann-Whitney Test; in the event of a significant difference ($p<0.05$), the condition is marked with a double asterisk (**).

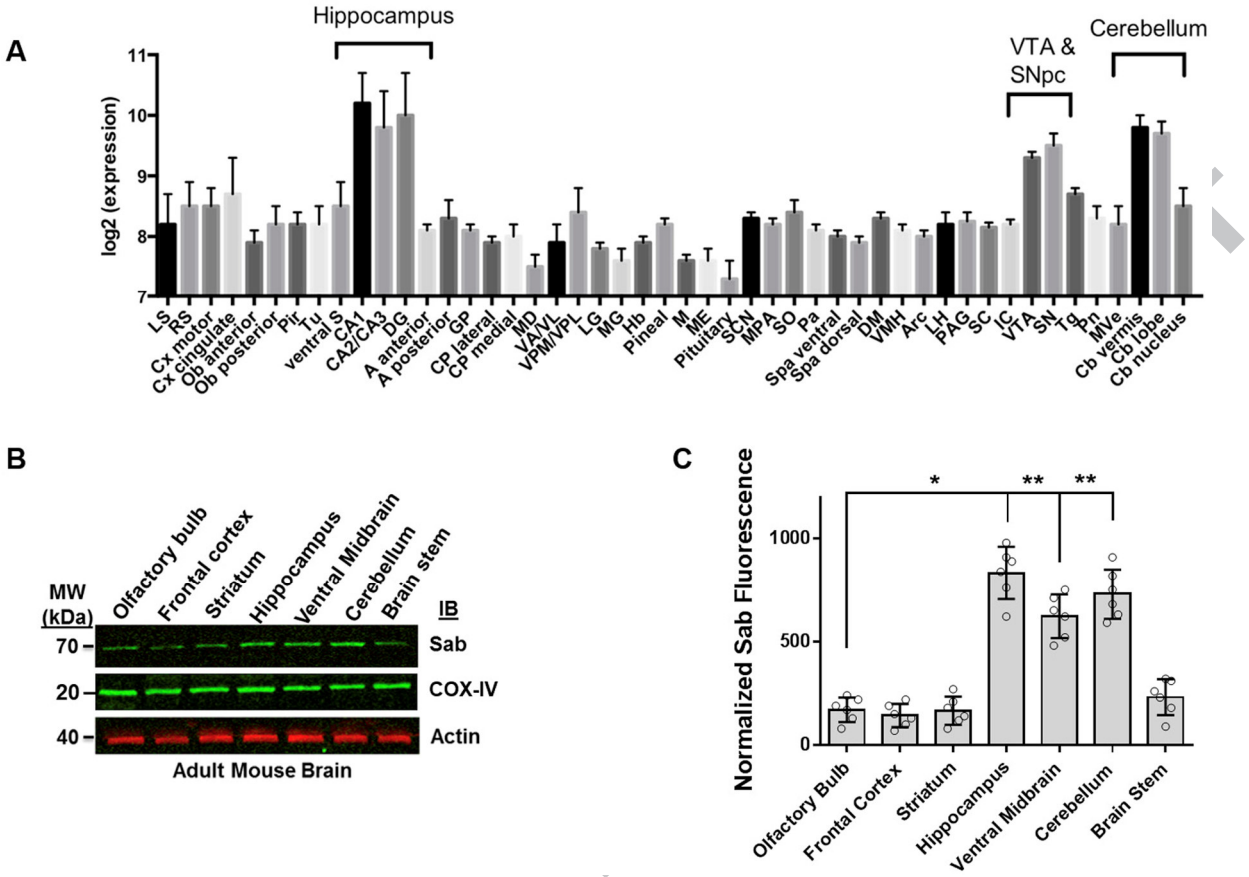

1

2

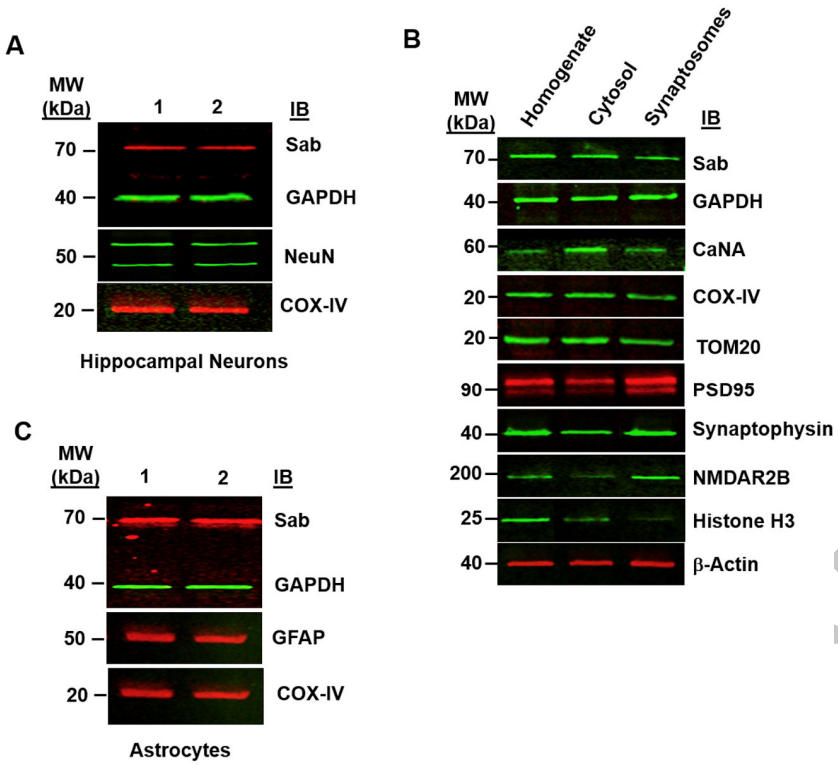

1

2

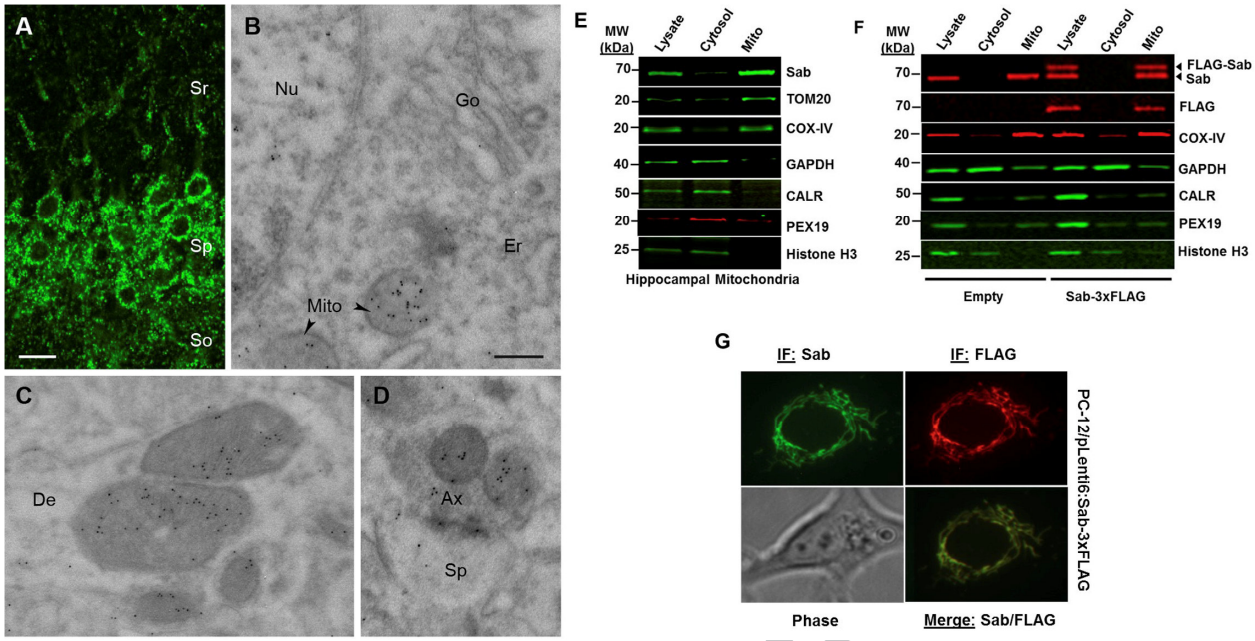

1

2

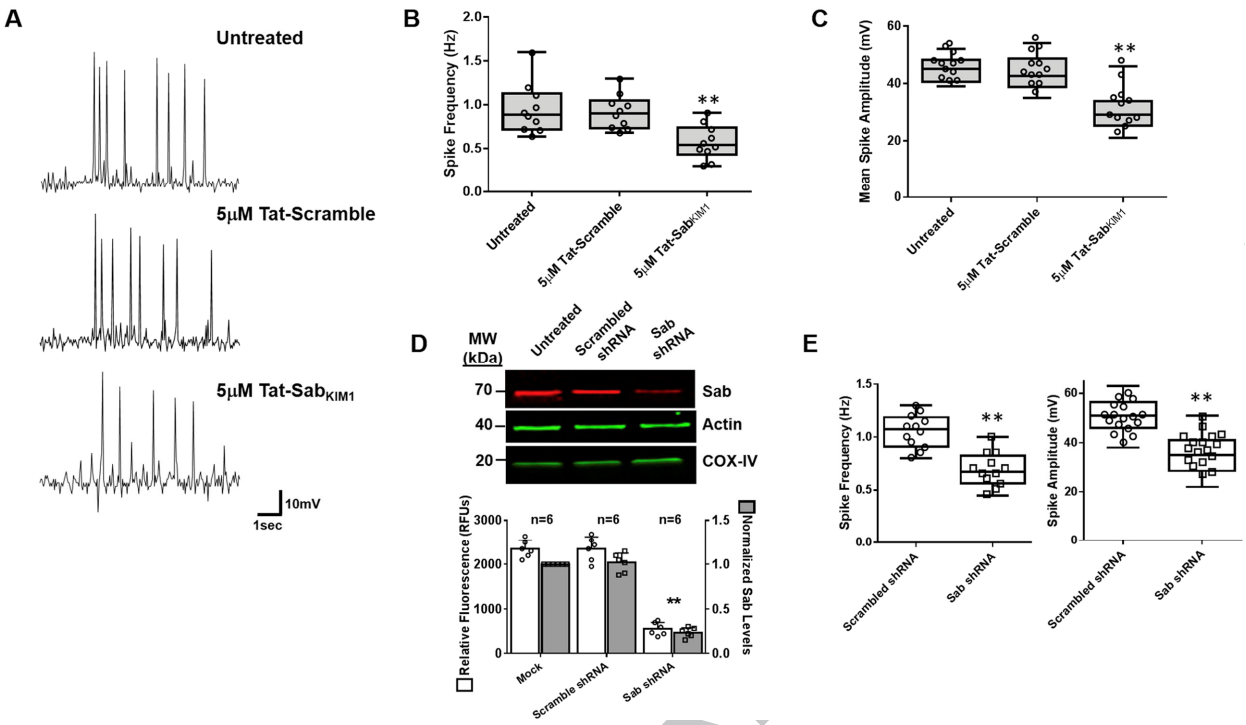

1

2

Highlights

- Sab, a mitochondrial scaffold protein for the c-Jun N-terminal kinase (JNK), is ubiquitously expressed in the adult brain.
- Sab has higher levels of expression in the cerebellum, hippocampus, and ventral midbrain.
- Sab can be found in mitochondria at synapses and in axons and dendrites.
- Inhibition of Sab-mediated events impairs neuronal activity.